

CONF-8505115-4

RECEIVED BY OSTI

MAY 06 1985

LA-UR--85-1138

DE85 010780

Los Alamos National Laboratory is operated by the University of California for the United States Department of Energy under contract W-7405-ENG-36

TITLE: Pattern Recognition and Tomography using Crosswell Acoustic Data

AUTHOR(S): James N. Albright
Darrell A. Terry
Christopher R. Bradley

SUBMITTED TO: SPE/DOE Joint Symposium on Low Permeability Reservoirs
May 19-22, 1985
Denver, Co

DISCLAIMER

This report was prepared as an account of work sponsored by an agency of the United States Government. Neither the United States Government nor any agency thereof, nor any of their employees, makes any warranty, express or implied, or assumes any legal liability or responsibility for the accuracy, completeness, or usefulness of any information, apparatus, product, or process disclosed, or represents that its use would not infringe privately owned rights. Reference herein to any specific commercial product, process, or service by trade name, trademark, manufacturer, or otherwise does not necessarily constitute or imply its endorsement, recommendation, or favoring by the United States Government or any agency thereof. The views and opinions of authors expressed herein do not necessarily state or reflect those of the United States Government or any agency thereof.

By acceptance of this article, the publisher recognizes that the U.S. Government retains a nonexclusive, royalty-free license to publish or reproduce the published form of this contribution, or to allow others to do so, for U.S. Government purposes.

The Los Alamos National Laboratory requests that the publisher identify this article as work performed under the auspices of the U.S. Department of Energy.

DISTRIBUTION OF THIS DOCUMENT IS UNLIMITED

 Los Alamos National Laboratory
Los Alamos, New Mexico 87545

PATTERN RECOGNITION AND TOMOGRAPHY USING CROSSWELL ACOUSTIC DATA

by J.N. Albright, D.A. Terry, and C.R. Bradley, Los Alamos National Laboratory

ABSTRACT

Measurements of the travel time of acoustic signals transmitted between wells at the Department of Energy Multi-Well Experiment site (MWX) near Rifle, Colorado, are processed and analyzed. Interpretations relevant to sand geometry and continuity have proved possible through inspection of the signal travel time plotted against the coordinates of transmitter and receiver wellbore positions, or against the depth of receiver and ray path inclination. The continuity of several sands between wells is corroborated. A major lenticular sand terminating between wells could be inferred.

To explore the possible distortions of tomographic images derived from crosswell data, synthetic tomographs are constructed from computed travel times of signals transmitted through idealized models from stratigraphy thought to be present at the MWX site. The synthetic tomographs, although preserving the general character of the model stratigraphy, are distorted enough that detailed interpretations are not possible. Horizontal distortions predominate in reconstructions of flat-lying stratigraphy.

INTRODUCTION

Increasingly geophysicists are evaluating the potential of crosswell measurements for the recovery of two-dimensional information about the structure and properties of rock between wells. At this time, significant advances in borehole instrumentation, data analysis, and computed "image" recovery and the interpretation of those images are required before crosswell acoustical surveying can be adopted as a useful tool in reservoir engineering.

This paper addresses two related subjects bearing on the status and prospects for crosswell imaging. First, we show that two-dimensional information about reservoir structure can be inferred from crosswell data displayed in an adaptation of the conventional

log format. Data can be displayed also by cylindrical coordinates of the transmitter referenced to the receiver. This display is called a gamma-depth (γZ) plot. Thus, the reliance on two-dimensional reconstruction images to interpret of crosswell data may not be as necessary as previously thought. Second, because crosswell measurement positions are limited to parallel or nearly parallel wellbores, potentially misleading distortions are introduced in computed images. Nonetheless important information can be derived about the properties of predominantly horizontal stratigraphy through the use of algebraic reconstruction technique (ART) codes in their present state of sophistication.

CROSSWELL MEASUREMENTS AT THE MWX SITE

The crosswell acoustic data reviewed here were acquired at the DOE Western Gas Sands Program -- Multi-Well Experiment (MWX) site near Rifle, Colorado. The goals and status of the MWX Project have been reviewed by Northrop et al.⁶ The crosswell surveys at Rifle were to provide information about the stratigraphy, structure, and physical properties of a complex sequence of gas-bearing sands and to gain experience in crosswell measurement methodology and data interpretation as applied to lenticular sands.

All measurements were conducted in the coastal zone of the Mesa Verde formation extending from approximately 6000 to 6800 feet. A crosswell survey consists of a collection of scans in which a repetitive signal source, or transmitter, is moved in one well between positions at comparable distances above and below the depth of a receiver stationed in a neighboring well. The movement of a transmitter in one well while receiving crosswell data in a second well is termed a transmitter run. The included angle between an imaginary line drawn between transmitter and receiver positions and the horizontal at the receiver is the ray path angle γ . Crosswell surveys were made between each MWX well (wells 1, 2, and 3). The wellbore separations at the study depths were 121, 221,

and 202 feet, respectively, for the well pairs MWX-1/2, MWX-2/3, and MWX-3/1. Before surveying commenced, wireline depths were calibrated against casing collar depths shown on commercial cement bond logs previously taken in the MWX wells. Transmitter runs were 240 feet for the MWX-1/2 survey and 120 feet for the MWX-2/3 and MWX-3/1 surveys. For the MWX-1/2 scans, γ was $+45^\circ$. Runs were made at rates of 60 feet/minute during which time the transmitter was fired at a rate of five signals/second or equivalently five signals/foot. The receiver remained stationary during scans in order to avoid unnecessary noise. Between scans the receiver was moved 5-feet vertically. Approximately 80,000 signals were transmitted between the wells in scans that comprise the crosswell surveys in the coastal zone.

The borehole tools used at the MWX site are an adaptation from commercial logging tool technology. The transmitter and receiver consist of a magnetostrictive scroll and a segmented piezoelectric crystal, respectively. Received signals transmitted between wells are bandlimited at ± 1 kHz and are centered at about 2.2 kHz. Because of the special nature of crosswell measurements, approximately an order of magnitude more energy can be discharged to the scroll, and receivers can be operated at roughly 20 dB greater sensitivity than that required by their industrial counterparts, which are used for sonic logging. Signal-conditioning electronics are deared and thermally buffered with heat sinks. Both transmitter and receiver are housed in centralized nonlocking tools and can be moved rapidly.

Representative crosswell scans are shown in Figure 1. The first signal to arrive at any depth is the P-wave or compressional-wave signal. The P-wave arrival shows hyperbolic moveout with respect to the signal transmitted the shortest distance between wells, which is approximately at the center depth of the scan. The loss in amplitude of signals at the top and bottom of transmitter runs is due to the combined effect of the intrinsic attenuation of signals along their propagation path, the reflection and scattering of signals at physical interfaces, the angular sensitivity of the receiver, and the radiation pattern of the transmitter. Depth intervals for which the amplitude of the P-wave arrival is uniformly high correspond to the depth of source/receiver ray paths predominantly through lenticular sands.

For the analysis which follows, signals transmitted over each 2-foot interval run, 10 in all, were stacked and plotted with expanded time and amplitude scales. P wave arrival times were determined by inspection, and actual picks were made using a digitizing platen.

PATTERN RECOGNITION

Important information about the geologic structure between wells can be extracted from crosswell scans without resorting to elaborate processing. Two representations of crosswell

data have proved useful. The first representation, the Crosswell Acoustic Velocity Log, displays the velocity of signals transmitted between wells in terms of the cartesian coordinates of the transmitter and receiver positions. In the second representation, the γZ plot, the travel time of signals transmitted between wells is displayed by cylindrical coordinates of the transmitter referenced to the receiver.

Portions of the Velocity Log for the coastal zone are shown in Figures 2a (top) and 2b (bottom). Each vertical panel corresponds to data collected in a single scan, that is, data collected for the transmitter run associated with one receiver position. The depth of the transmitter increases from top to bottom in each panel. Receiver depth changes incrementally from panel to panel. Thus, the Log displays the velocity of signals transmitted between all combinations of transmitter and receiver positions.

The principal sands in the Velocity Log appear as smooth, slightly higher than average velocity intervals. Boundaries between thick sands and distinctly more heterogeneous stratigraphy can be seen in several adjacent panels. Calculations of synthetic velocity data based on geometric simplifications of common stratigraphy provide suggestions concerning the significance of these and other boundaries that may be observed in Velocity Logs. Although Synthetic Logs can be computed in a much more sophisticated manner than what follows, the logs presented are sufficient to illustrate the concept that stratigraphic interpretations are possible based on the pattern of boundaries observed in Velocity Logs.

In Figure 3 Synthetic Logs (bottom) and their respective stratigraphic models (top) from which they were computed are given. The Synthetic Logs are for strata with small velocity contrasts so that a straight-ray path approximation can be used in calculating the travel time of signals transmitted between wells. The square gray-tone fields represent log subsections in the range where transmitter and receiver depth overlap completely. High velocity in the model is represented by dark gray, and high velocity in the transmitter vs. receiver plot is white. The Synthetic logs shown are for

- (I) a sand channel present between wells but not penetrated by either,
- (II) a sand penetrated by only one well and terminating between wells,
- (III) a sand which is continuous between wells,
- (IV) a sand faulted between wells, and
- (V) a sand discontinuous between wells but penetrated by both.

Geophysical logs alone should allow the inference of the Type II or III stratigraphy between wells. Types I and V are common stratigraphy for channel sands, but they cannot be detected by geophysical logs. Whether Type IV could be inferred from borehole logs is problematical. Evidence of faults with small offsets between wells may easily escape detection in complex stratigraphic environments.

Synthetic Log patterns are substantially different for each stratigraphic or structural type. Only in Type III does the boundary between high and low velocity occur at either constant receiver or transmitter depths. The remaining types have at least one sloping boundary in terms of transmitter and receiver coordinates. Sometimes complete patterns are not observed in actual logs; therefore, an interpretation based on Velocity Log data will be non-unique unless the interpretation can be constrained by geophysical logs. Because the boundaries designated as "unidentified sand" and "Red Sand" in Figure 2 display a negative slope, a Type III interpretation is not allowed. Further, because the first sand is not represented in borehole logs taken in either well, we must conclude that the boundary arises from a structure similar to the Type II stratigraphy, possibly a channel sand. An inspection of the geophysical logs for both wells confirms the existence of the "Red Sand". In this instance a IV or V type structure or a variation thereof is implied.

An alternative representation of crosswell travel-time data, the gray-tone or contoured display, is plotted against the receiver depth Z and the ray path angle γ . Figure 4 shows the relationship between crosswell survey geometry and γZ plots. Gray-tones represent velocity contrasts; e.g., lighter shades show higher velocity and vice versa. Gray-tones parallel to the Z -axis (right) represent the relative travel time of signals between receiver and transmitter positions having constant γ_0 (left). Gray-tone perpendicular to the Z -axis gives the relative travel time of all signals between wells in a single scan (γ_0 to γ_1). The centerline $\gamma = 0$ corresponds to the travel-time of signals transmitted horizontally between wells. Figures 5 and 6 are γZ plots of the actual data, and Figures 7a and 7b represent a model based on the data.

Suppose, for argument, the model stratigraphy occurs in a structural environment where its vertical extent is dependably represented in geophysical logs but its continuity between wells can be challenged. If we assume that data from a crosswell acoustic survey are available, what evidence for stratigraphic continuity between wells can be found in γZ plots? To address this question, the γZ pattern in a horizontal stratigraphic model of the MxX coastal zone (Figure 7a) was calculated; Small velocity contrasts between the strata and a straight-ray path signal propagation were assumed. The result, which is generally applicable to any horizontal stratigraphy, is given in Figure 7b. A

stratigraphically continuous bed appears in γZ plots as an uninterrupted sloping "bow-tie" travel-time anomaly, as seen in the top of Figure 7b. The negative slope of all the anomalies occurs because, for receiver positions above the stratum, no ray path having a positive take-off angle will penetrate the strata; For receiver positions below the stratum, the converse is true. The thickness of the knot in the "bow-tie" at 0° corresponds to the thickness of the bed.

Measured travel times of signals transmitted between wells through the coastal zone are shown in Figures 5 and 6 as gray-tone and contour γZ representations, respectively. Two major travel-time anomalies are evident. The lowermost appears to have three subsidiary divisions. Figure 7a and its γZ representation in Figure 7b show that both anomalies arise from acoustic contrasts that are stratigraphically continuous between wells.

Sonic and neutron density geophysical logs indicate that the lowermost units are coals interrupted by mixed shale/sandstone stratigraphy. The uppermost anomaly has no apparent expression on geophysical logs. Core and geophysical logs indicate that the stratigraphy at the depth of this anomaly is interbedded fluvial shales and sands rather than a single thick sand. This anomaly probably represents a significant change in formation properties superimposed on a heterogeneous lithology.

LIMITED APERTURE TOMOGRAPHS

Since the ray path angle in crosswell surveys seldom exceeds $\pm 45^\circ$, sufficient data can be acquired to compute exact images of acoustic properties between wells. In attempting to algebraically reconstruct a velocity image from a crosswell survey, the computational steps are the following:

- (i) a starting image (stratigraphy) is assumed;
- (ii) the travel times for all signals transmitted through that image are predicted;
- (iii) predicted and travel times measured in crosswell surveys are compared, and
- (iv) differences in travel time found in that comparison are used to improve the current image before repeating steps (ii), (iii), and (iv).

The starting image may be a "best guess" of the tomographic image one seeks to reconstruct, or commonly, an image having a constant velocity view is used. The final image shows the variations in travel time across cells that spatially fill the image. A velocity image can then be directly calculated from a travel time image.

By making tomographic reconstructions for which exact images or constant velocity images are initially assumed, one finds the least and greatest distortions in final calculated images that will occur using any particular calculational scheme. In computing tomographs using actual crosswell data, image distortion will probably lie between the two extremes. Beneficial starting images can be constructed using data derived from wellbore geophysical logs and models based on stratigraphic interpretations. The advantage gained from logs and stratigraphic models must be weighed against the effects of measurement error.

An industrial imaging code adapted to the geometry of crosswell surveys was used to study the effect of the limited range of ray path angles available for image reconstructions. The code belongs to a class commonly called ART or the Algebraic Reconstruction Technique. Only small velocity contrasts are considered so that the straight-ray path approximation may be assumed for the coastal zone measurements, the maximum range in γ (the aperture) is approximately 90° . In crosswell surveys between distant wells, γ will be considerably less.

The images shown in Figure 8 were calculated for a rectangular object in the center of a field of view having a γ range of 180° to 60° . The reconstructions were made using constant-velocity starting images. With decreasing γ the amplitude and orientation of the distortions change. Another set of calculations (not shown) was made in which a rectangular analogue of a sand channel was rotated in the field of view having a 90° range in ray path angle. Distortions in boundaries were the smallest parallel to the wellbores. The shape of the channel was best resolved when the channel was tipped 45° on its side. Thus, highly dipping structural features located between wells will be least resolved by crosswell measurements.

Figure 9 shows an image reconstructed (bottom left) from synthetic travel times derived from a simplified velocity model of the coastal zone sand stratigraphy (top left). For simplicity, the coastal zone is separated exclusively into sand and "other" stratigraphies and a constant velocity is assigned to each. The "other" stratigraphies (coals, shales, and minor sands) are thin interbedded layers which are highly variable in velocity. Hence, one can expect that, in recovering the image of the coastal zone using real data, the major sands will stand out against a chaotic background as broad regions of slowly varying velocity. In this case, one may have obtained a poor image of the fine structure of the coastal zone but nevertheless generated an acceptable image of the gas-bearing sands, the latter being the sought after result.

The travel time of signals transmitted between wells through the model sand stratigraphy was calculated to provide synthetic

data with which to evaluate the ART. The reconstruction was calculated from the synthetic data; a γ range of 90° and a constant velocity starting model were assumed. The correspondence between the model and the reconstruction is generally good. Although details in the model are not faithfully recovered in the reconstruction, information about continuity or lack of continuity of sands is preserved. The prospect for recovering useful information from crosswell surveys appears good; however, the distortions introduced during image reconstruction, as well as the inherent heterogeneity of the stratigraphy of potential interest, present a challenge to interpretation.

CONCLUSIONS

1. Representations of the travel times of P-waves transmitted between wells, in terms of the source and receiver coordinates, provide useful information about the structure and properties of rocks between wells. The recognition of patterns in those representations that are characteristic of common geological stratigraphy and structure will facilitate their interpretation.
2. The range in ray path angles is limited in crosswell surveying. This characteristic distorts computed images of the velocity structure between wells. Contemporary ART codes provide computed images derived from crosswell data that preserve the general structural character of the surveyed rock. However, detailed interpretations based on the images are not now possible.

NOMENCLATURE

- γ angle measured positive from horizontal
 Z depth (ft)

ACKNOWLEDGMENTS

The development of crosswell acoustic measurements as a diagnostic tool for reservoir engineering is supported by the Department of Energy Western Gas Sands (WGS) Program. The Earth Sciences Instrumentation Group at Los Alamos National Laboratory designed, fabricated, and fielded the borehole tools used to conduct the crosswell surveys.

The authors wish to express their appreciation for the encouragement and logistical support provided by Karl-Heinz Frohne, WGS Program Manager, and David Northrop and Robert Mann, MWX Project Managers. Also, we are indebted to Ken Hansen for his help in the understanding and use of the tomographic code.

REFERENCES

1. Lytle, R.J., and Dines, K.A., "Computerized Geophysical Tomography," Proc. IEEE, 67, 1065-1073, 1979.

2. Albright, J.N., Pearson, C., and Fehler, M., "Transmission of Acoustic Signals Through Hydraulic Fractures," SPWLA 21st Annual Meeting Proc. Paper R, 1980.
3. Kretzschmar, J.L., and Witterholt, E.J., "Enhanced Recovery Surveillance Using Well-to-Well Tomography," Proceedings of the SPE/DOE Fourth Symposium on Enhanced Oil Recovery, SPE/DPE 12680, 1984.
4. McMechan, G.A., "Seismic Tomography in Boreholes," Geophys. J.R. Astr. Soc., 74, 601-612, 1983.
5. Wong, J., Hurley, P., and West, G.F., "Crosshole Seismology and Seismic Imaging in Crystalline Rocks," Geophys. Res. Lett. 10, 686-689, 1983.
6. Northrop, D.A., Sattler, A.R., and Westhusing, J.K., "Multi-Well Experiment: A Field Laboratory for Tight Gas Sands," Proceedings of SPE/DOE Symposium on Low Permeability Gas Reservoirs, SPE/DOE 11646, 1983.
7. Lorenz, J.C., "Predictions of the Size and Orientation of Lenticular Reservoirs in the Mesa Verde Group, Northwestern Colorado," Proceedings of SPE/DOE Symposium on Low Permeability Gas Reservoirs, SPE/DOE 13851, 1985.

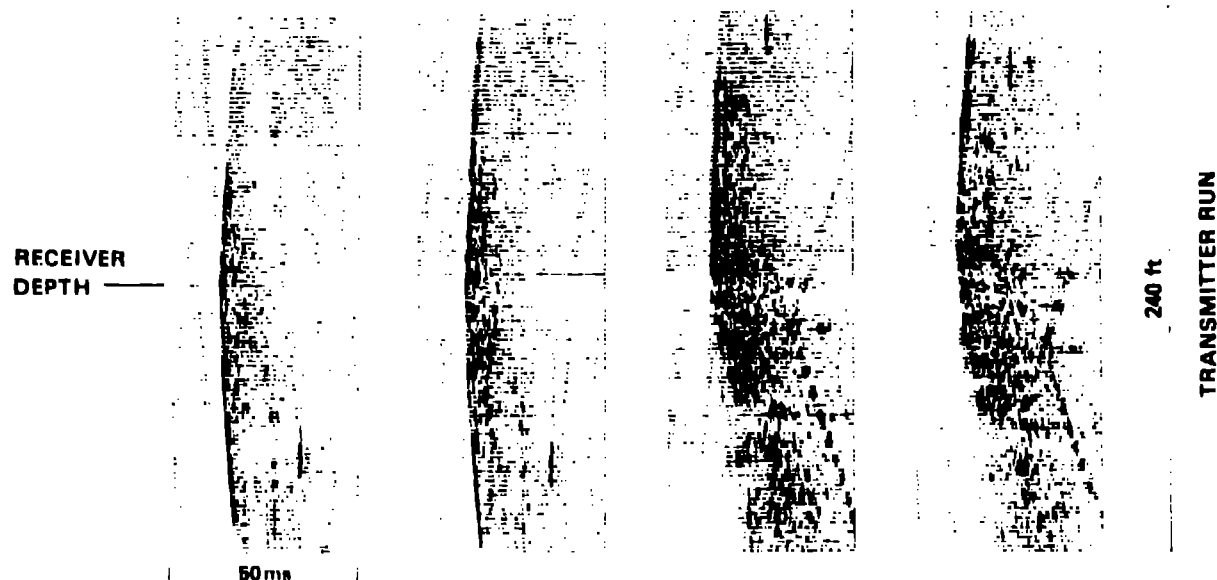


Fig. 1. Crosswell scans at receiver depths of (a) 64.0', (b) 64.30', (c) 66.0', and (d) 66.10 ft.

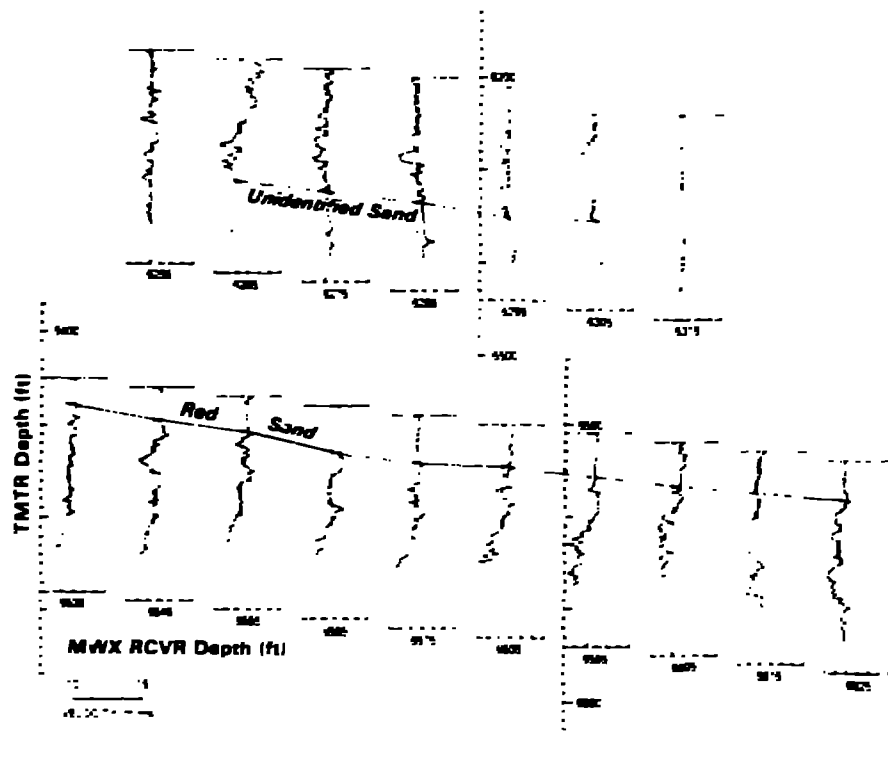


Fig. 2. Sections of a Crosswell Acoustic Velocity Log showing an isolated sand channel (top) and a discontinuous lenticular sand (bottom).

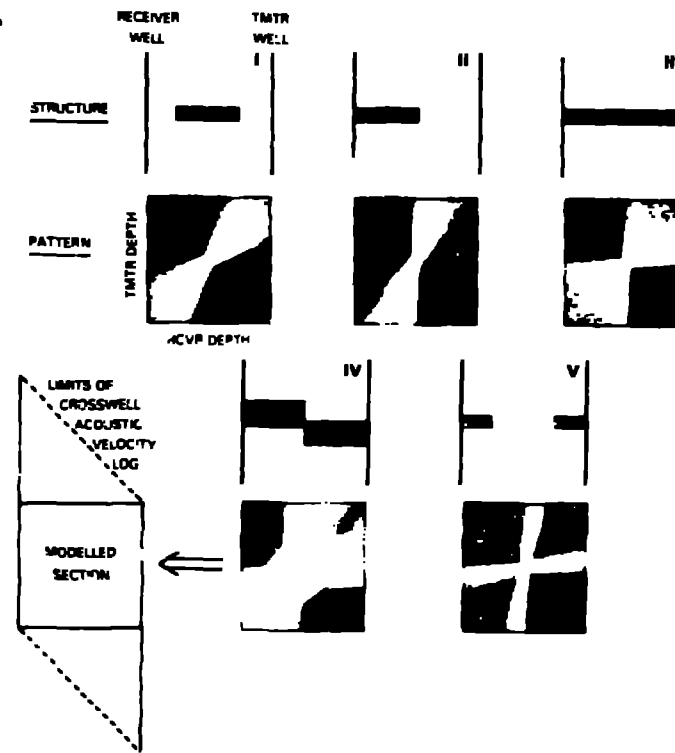


Fig. 3. Velocity Log Patterns. High relative velocity in the model is dark gray; while in the pattern plot, high relative velocity is white.

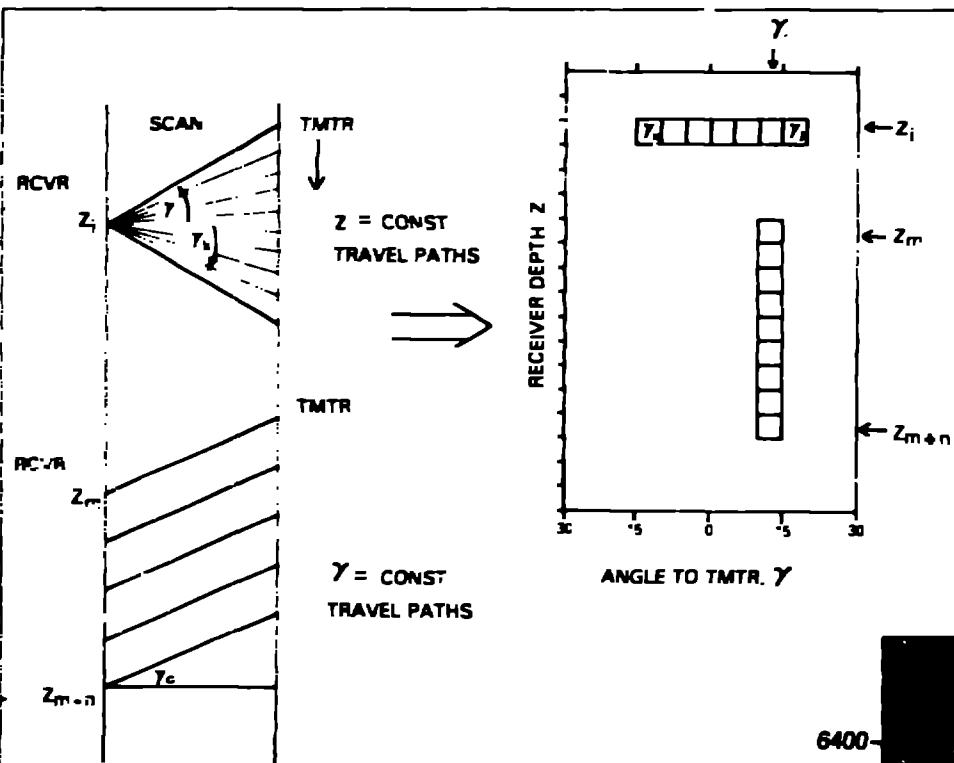
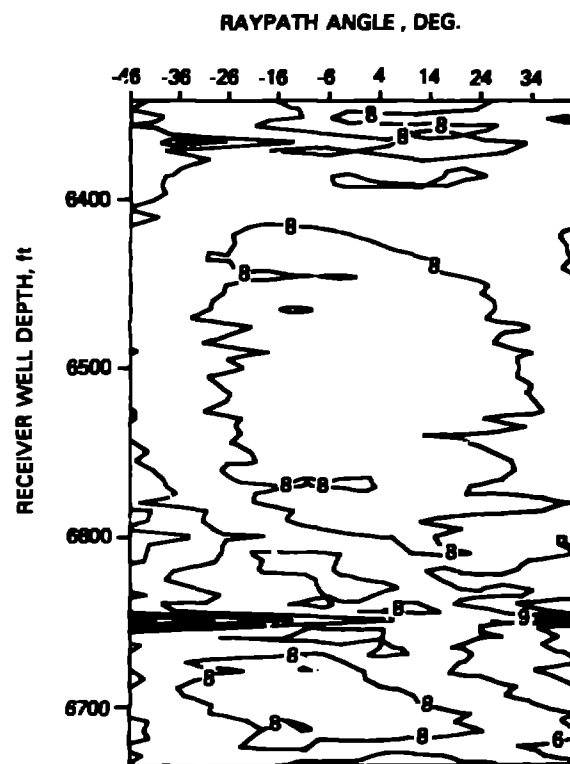
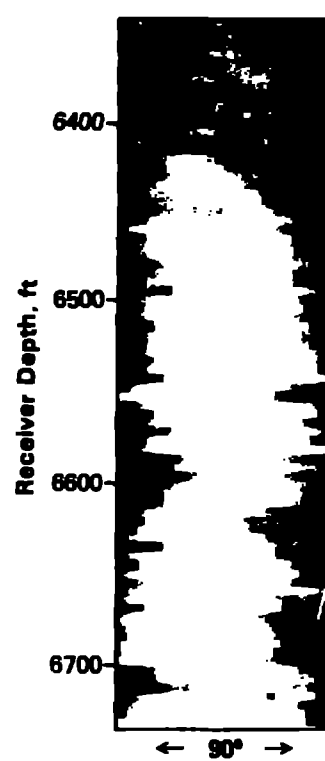


Fig. 4. Relationships in yZ plot of P-wave travel times. Travel times of an entire scan represented by γ_1 to γ_k in the top of the figure at left are plotted horizontally at a given receiver position (Z_i) in the right-hand figure. Consecutive receiver positions at a constant angle γ_c between Z_{m+n} to Z_m (left) are plotted vertically at right.

Fig. 5. Gray tone yZ plot of F-wave travel times measured in the MWX 1/2 survey. Lighter tone equals high velocity.

Fig. 6. Contour plot of the travel time data presented in Fig. 5. Numbers on contours indicate travel time in ft./sec.



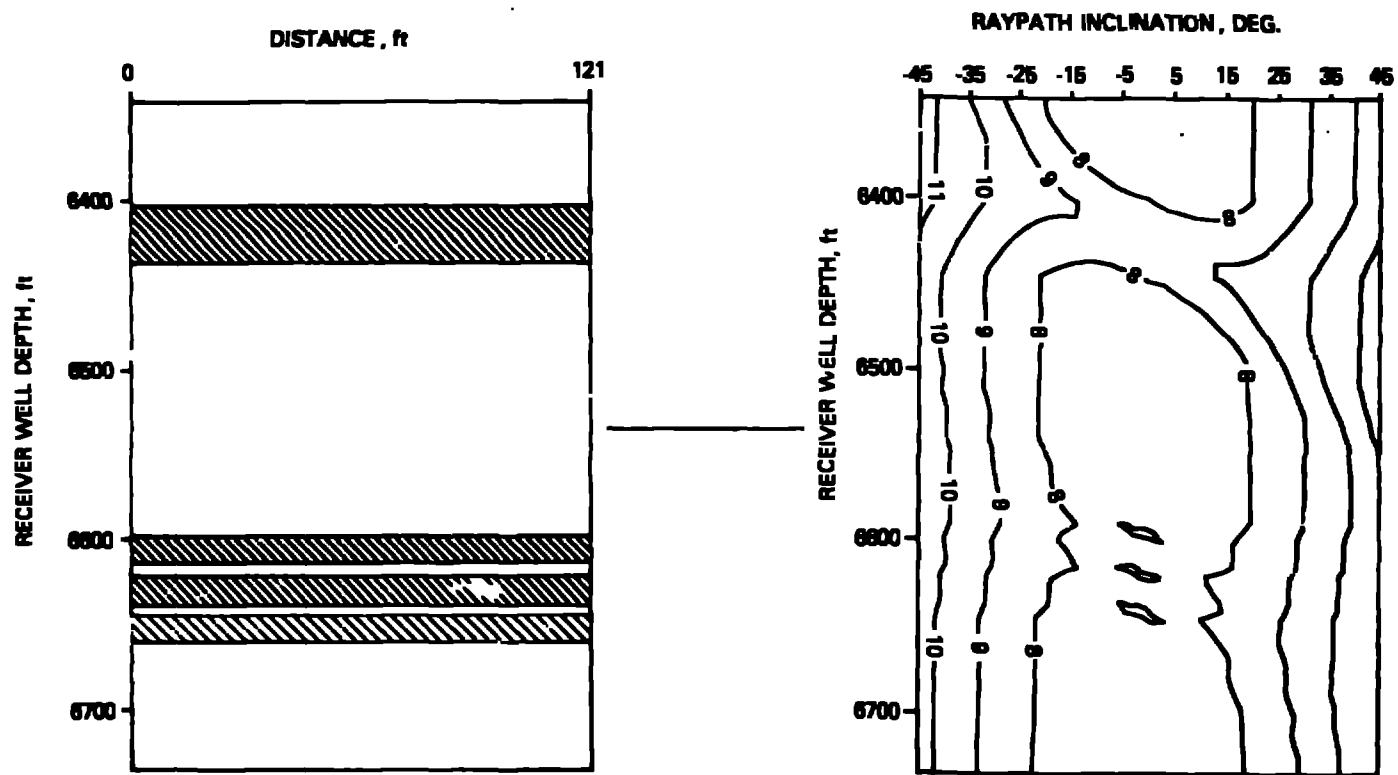


Fig. 7. (a) Velocity model used in synthetic travel-time calculations for contoured T_Z plot of (b) resulting synthetic travel-time data. Contour units are ft/msec.

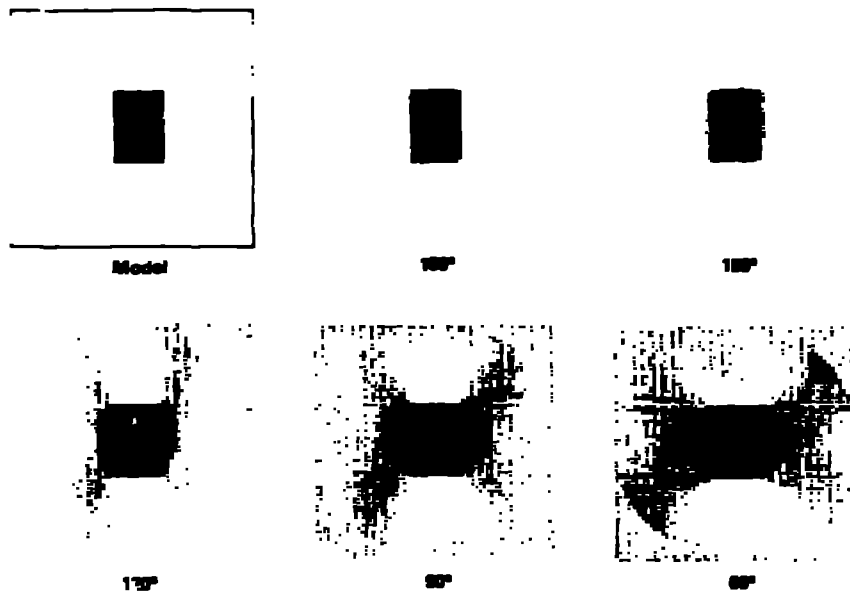


Fig. 8. Effect of a limited range in ray path inclination on tomographs of a simple model.

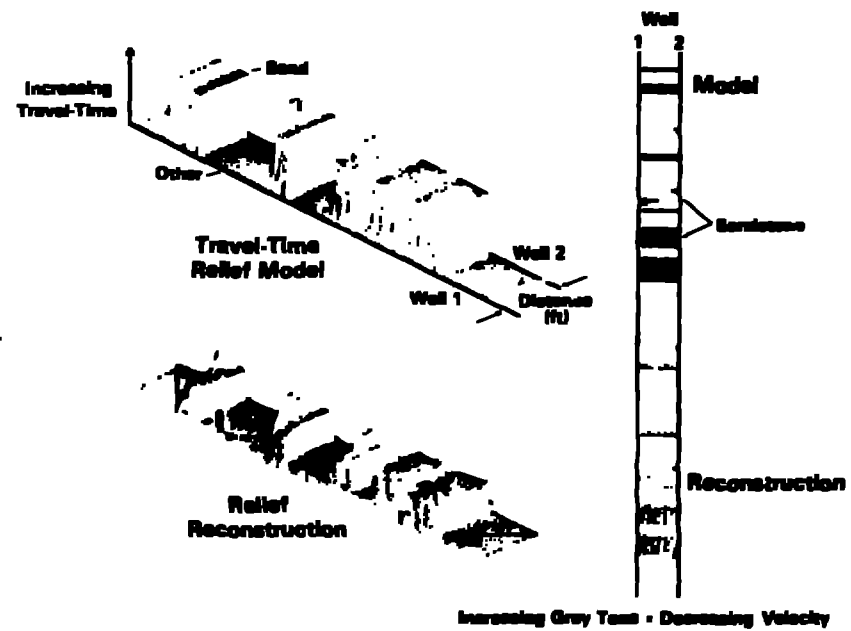


Fig. 9. An ART reconstruction of a simplified sand stratigraphy using a range of 90° in ray path angle and synthetic travel-time data.